Efficient charge storage in photoexcited TiO_2 nanorod-noble metal nanoparticle composite systems†

P. Davide Cozzoli,*[a] M. Lucia Curri[b] and Angela Agostiano[ab]

Received (in Cambridge, UK) 15th March 2005, Accepted 29th April 2005
First published as an Advance Article on the web 24th May 2005
DOI: 10.1039/b503774c

Following UV-illumination, TiO_2 nanorod-stabilized noble metal (Ag, Au) nanoparticles dispersed in deaerated organic mixtures can sustain a higher degree of conduction band electron accumulation than that achievable with pristine titania.

Developments of innovative technologies and devices based on the size-dependent physical-chemical properties of semiconductor nanoparticles (NPs) rely on the ability to control the various relaxation processes through which excitons decay.[1] A fundamental challenge in modern quantum dot chemistry is to realize either opposite situations. At one extreme, efficient radiative electron–hole recombination and suppression of redox reactions at the NP surface are desirable to guarantee maximum band-edge luminescence;[2] on the other hand, carrier separation needs to be enhanced when aiming for the extraction of chemical energy.[3–5] Indeed, exciton break-up provides the basis for performing photocatalytic reactions,[3] for realizing dye-sensitized solar cells,[4] and for the operation of charge storage devices.[5,6]

In conventional steady-state photocatalysis, it is generally desirable to minimize accumulation of photogenerated conduction band (CB) electrons (e_{CB}) on the semiconductor,[15] because rapid reaction of the nascent holes with the resident excess e_{CB} would likely prevail over subsequent exciton break-up. As opposed, in charge storage schemes, rapid and quantitative transfer of one of the carriers to a solution-phase redox couple is usually required to build up a net e_{CB} charge.

A variety of electrochemical,[5–7] photochemical,[8] and catalytic[9] experiments have highlighted that noble metal (*e.g.* Ag, Au, Pt) clusters exhibit unusual size-dependent redox activity[5–9] by readily storing electrons in a quantized manner[5] and favouring their subsequent release to suitable acceptors. Based on these unique properties, metal NPs have been commonly coupled to semiconductor oxides (*e.g.* TiO_2 and ZnO) to facilitate the shuttling of the photoexcited e_{CB} to solution species. This association can improve photocatalytic performances owing to charge carriers escaping recombination.[10–15]

In general, only composite systems establishing ohmic metal–solution contact act as efficient catalysts for quick e_{CB} migration to the solution (this is the case of Pt or Pd). Conversely, in the presence of non-ohmic interfaces (*e.g.* with Ag, Au, Cu), excess e_{CB} can remain stored effectively on both components of the nanojunction under suitable conditions.[11–14] Upon sufficient charge accumulation, the Fermi levels of the two components can equilibrate at a potential that is progressively shifted to more negative values with increasing electron density.[13,14] This altered energetics plays a fundamental role in modulating the overall photocatalytic activity of semiconductor–metal composite systems,[10–15] although the detailed mechanism of interfacial electron transfer processes remains to be fully clarified.

The present work demonstrates the improved e_{CB} storing ability of photoexcited TiO_2 nanorod (NR)-stabilized metal NPs[16–18] as compared to that achievable with the sole oxide NRs, and the feasibility of extracting the trapped electrons for efficient reductive reactions. The system under investigation consists of either photocatalytically generated Ag[17] or Au[18] NPs, whose colloidal stabilization in nonpolar solution is achieved exclusively by means of electrostatic interactions with surfactant-capped anatase TiO_2 NRs. While remaining heterogeneous at the nanoscale, the nanocomposite solution keeps optical transparency, which allows for the real-time spectrophotometric monitoring of any metal–TiO_2 (photo)catalyzed reaction course.[15] In addition, such NR-stabilized Ag/Au NPs possess a virtually "clean" surface, *i.e.* not passivated by organic ligands having affinity to the metal.[17] Because of this unique feature, metal-mediated reductive reactions can be performed in the absence of capping agents preventing the access of molecular species to the metal surface and/or interfering with electron transfer processes. Therefore, probing the trapped charge by reacting e_{CB} with a suitable acceptor can provide a comparative evaluation of the intrinsic e_{CB}-storing properties of the TiO_2–metal composites as a function of the metal type.

The effect of metal–semiconductor association was studied under charge equilibrium conditions. UV-photoexcitation (λ = 254 nm, 400 $\mu W\ cm^{-2}$)† of TiO_2 NRs dissolved in N_2-saturated $CHCl_3$–EtOH mixtures resulted in accumulation of conduction band electrons at Ti(IV) sites.[19] This phenomenon was marked by a distinguishable absorption extended up to the near-IR region, as shown in Fig. 1. Admission of air to the solution instantly quenched the blue coloration, as the stored electrons were scavenged by O_2, whereas recovery of the initial spectrum took several hours (8–12 h) under inert atmosphere, due to the slow e_{CB} release to the solution.

The growth kinetics and the final intensity of e_{CB} absorption depend on the experimental conditions, such as light intensity, irradiation time, TiO_2 concentration, and solvent nature. The latter parameter is even the most critical in promoting the blue coloration. Although in chloroformic media the photogenerated electrons are short-circuited in the TiO_2-photocatalyzed reductive degradation of $CHCl_3$,[15,20] adjustment of the solution composition to suitable $CHCl_3$:EtOH ratios† can facilitate their accumulation on the semiconductor, due to efficient hole scavenging by ethanol.[19] However, a limitation of this approach is that optical

---

† Electronic supplementary information (ESI) available: experimental details on the preparation and TEM characterization of TiO_2 nanorod-stabilized Au and Ag NPs and on the photocatalytic experiments. See http://www.rsc.org/suppdata/cc/b5/b503774c/

*d.cozzoli@ba.ipcf.cnr.it

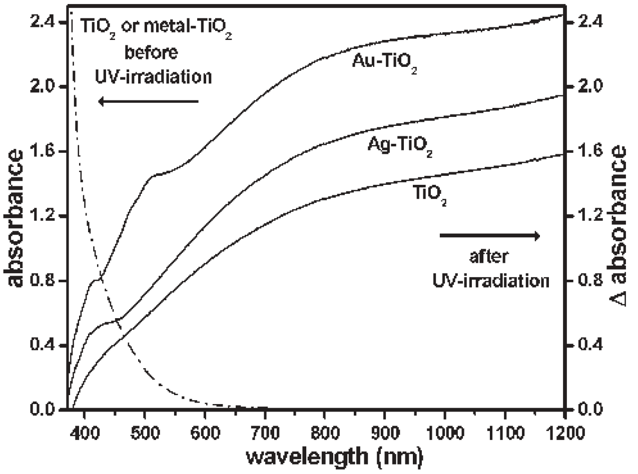

Fig. 1 Absorption changes (right axis, solid lines) upon band-gap photoexcitation of TiO_2 NRs and TiO_2 NR-stabilized metal NPs in O_2-free $CHCl_3$:EtOH = 60:40 v/v ([TiO_2] = 0.1 M, NR size: 3 nm × 25 nm, [metal] = 10^{-6} M, metal size: 15 ± 3 nm, 30 min irradiation at λ_{ex} = 254 nm). The spectra after illumination were taken using the unirradiated solution (left axis, dotted line) as the reference.

transparency can be preserved within a restricted composition range, as excessive alcohol content makes the hydrophobically-coated TiO_2 NRs loose their colloidal stability by nonsolvent effects, ultimately resulting in the co-precipitation of the metal component.[17,18]

As demonstrated by Fig. 1, the presence of either nearly spherical Ag or Au NPs with similar mean size and size-variance† affected the e_{CB} storage behavior of TiO_2 NRs dramatically. The higher absorption intensity in the difference spectra at any $\lambda > \sim 600$ nm indicated that the nanocomposite worked as a more efficient e_{CB} reservoir than the pristine oxide. Such an effect was enhanced by increasing NP concentration and/or decreasing the mean NP size and appeared more pronounced for TiO_2 coupled with Au than with Ag at constant metal concentration.† Unfortunately, due to the high TiO_2:metal ratio and to the low absolute metal content, the surface plasmon (SP) features of the metals were hardly distinguishable in the spectrum of pure TiO_2 before illumination (Fig. 1). Following photoexcitation, minor absorption changes at $\lambda = \sim 420$ nm for Ag–TiO_2 and at $\lambda = \sim 540$ nm for Au–TiO_2, respectively, could be consistent with metal charging.[5c,9a,10,11,17] The optical attributions were further supported by transmission electron microscopy (TEM) studies, confirming that the initial uniform separation of the metal NPs and their structural features were retained under the employed illumination conditions. Thus, possible absorption contributions at $\lambda > \sim 600$ nm arising from either size-morphological light-induced modification of the metal NPs[17] or from their self-assembly into chain-like aggregates[18] were ruled out. Finally, metal–semiconductor Fermi level equilibration was independently confirmed (data not shown) by injection of either unphotolyzed TiO_2 NRs or TiO_2 NR-stabilized metal NPs to pre-irradiated TiO_2: a higher decrease in the e_{CB} absorption was obtained in the latter case, which corroborated the hypothesis of transfer of a e_{CB} fraction to the metal NPs.

To further confirm the above assumptions, quantitative estimation of e_{CB} accumulation was performed by titrating excess TiO_2 electrons with Uniblue A (UBA). UBA, an antraquinonic dye† with an intense double absorption band at around 600 nm, is a convenient substrate to this purpose, as it exhibits remarkably modified absorption features when it is reduced to its hydroantraquinonic form.[15] Thus, known amounts of a concentrated O_2-free UBA solution were injected in small increments into the UV-irradiated nanocomposite solution and the difference spectrum was recorded after each addition. In the representative example of Fig. 2, any absorbance bleaching observed $\lambda > \sim 700$ nm reflects the progressive consumption of the trapped electrons in the reduction process, while the concomitant growth of characteristic bands at $\lambda < 500$ nm accomplishes the formation of UBA by-products. The appearance of the unreduced dye double band peaking at $\lambda' = 588$ nm and $\lambda'' = 625$ nm indicates that the e_{CB} reservoir has been depleted completely. Previous interpretation of the spectrophotometric data in Fig. 1 is therefore in agreement with the representative results of titration for TiO_2 and for metal–TiO_2 coupled systems summarized in Fig. 3. In the plot, the difference (ΔA) between the initial (*i.e.* following photolysis) absorbance value at $\lambda = 900$ nm, A_0, and that measured after each UBA addition is plotted *versus* the respective amount of added UBA. For each catalyst, the titration endpoint is located at the intersection point between the oblique and the horizontal portion (where obviously $\Delta A = A_0$) of the curve. The slope of the oblique line, that corresponds to $\varepsilon_e * 1/n$ (where ε_e = extinction coefficient of trapped e_{CB}, and n = number of electrons/dye molecule involved in the reduction) changes according to the order: $TiO_2 <$ Ag–$TiO_2 <$ Au–TiO_2. This should be a consequence of the modified e_{CB} storing properties of TiO_2 arising from its coupling with the different metals. More importantly, the total amount of UBA required for consuming the accumulated electrons increases according to the same order above. Thus, enhancement of reduction yield scales with the e_{CB} storing capability of the

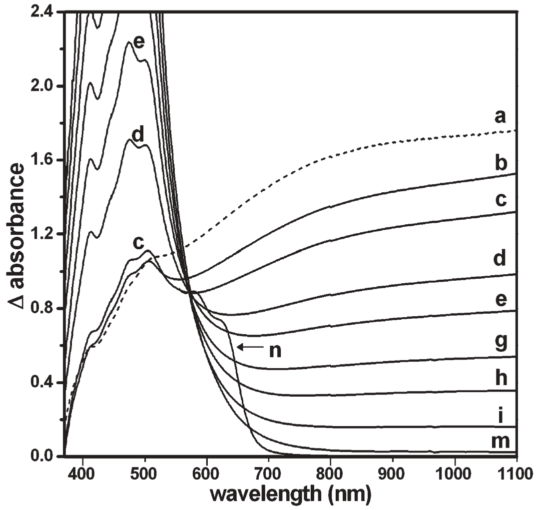

Fig. 2 Absorption changes occurring to UV pre-irradiated TiO_2-stabilized Au NPs (*a*) upon successive additions (5 μM each) of UBA under O_2-free conditions (*b–m*). When all stored electrons are consumed, the absorption features of unreduced UBA can be observed in spectrum *n*. Conditions: [TiO_2] = 0.1 M, NR size: 3 nm × 25 nm, [Au] = $5*10^{-7}$ M, metal size: 15 ± 3 nm; pre-irradiation time: 30 min. The spectra were taken using the unirradiated photocatalyst solution as the reference.

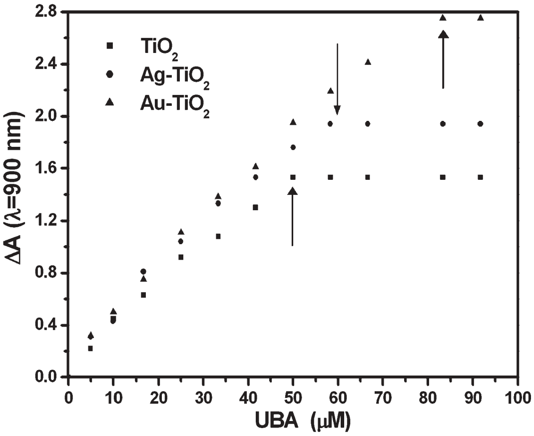

Fig. 3 Absorbance difference at $\lambda = 900$ nm after successive additions of UBA to UV pre-irradiated TiO_2 or TiO_2-stabilized metal NPs under O_2-free atmosphere. Conditions: $[TiO_2] = 0.1$ M, NR size: 3 nm × 25 nm, $[\text{metal}] = 5*10^{-7}$ M, metal size: 15 ± 3 nm, pre-irradiation time: 30 min). The arrows indicate the respective titration endpoints.

photocatalyst, being actually higher for the nanocomposites relative to the sole oxide.

The electron storage–release processes are summarized by the energetic diagram in Fig. 4. The position of Fermi level, E_F, in an open-circuit TiO_2 NP is dictated by the most facile redox couple present in the solution (dotted line). If the photogenerated holes are scavenged by the solvent, excess photogenerated electrons can accumulate in the oxide (blue-color of the colloid), and the Fermi level moves up (Fig. 4b) toward the CB edge ($E_{CB} = -0.5$ V *vs* NHE). In the presence of either Au or Ag, the electrons can flow from TiO_2 to the metal where they can accumulate. The metal Fermi level (dashed line) shifts cathodically, until it equilibrates with that of TiO_2 (Fig. 4c). In the presence of better acceptors than the solvent molecules, the metal NPs can then release the trapped electrons.

In the present system, the role played by the metal NPs can be twofold. First, the metal NPs possess the unique ability to store CB electrons. Although the latter distribute between both components of the composite system, at equilibrium excess e_{CB} density can reside overwhelmingly on the metal because the Helmholtz capacitance of the metal–solution interface is much higher than the space charge capacity of the semiconductor, even under accumulation.[11–14] This fact explains why metal–TiO_2 composite systems can sustain a higher degree of e_{CB} accumulation. Second, Au NPs should act as poorer catalysts for e_{CB} release to the solvent than the Ag NPs in order to maintain a higher net charge amount. This fact implies that the overall effect of metal coupling is dictated by the balance between the intrinsic e_{CB} storing ability of the metal and its efficiency in discharging e_{CB} to the solution.

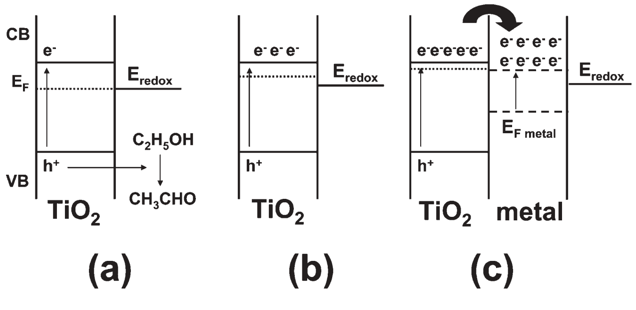

Fig. 4 Scheme of energy levels in TiO_2 before (a), and after photoirradiation either in the absence (b) or in the presence of metal NPs (c).

In conclusion, it has been demonstrated that, upon titania photoexcitation, TiO_2 NR-stabilized noble metal NPs behave as more efficient e_{CB} accumulators than the bare oxide. Therefore, such nanocomposites represent convenient systems to convert photochemical energy into the form of stored e_{CB}, which could pave the way to realize novel charge-storing nanodevices as well as to provide alternative electron sources for reagentless reductions.

The partial support of the EC-funded project NaPa (Contract no. NMP4-CT-2003-500120) is gratefully acknowledged.

P. Davide Cozzoli,*[a] M. Lucia Curri[b] and Angela Agostiano[ab]
[a]*Dipartimento di Chimica, Università di Bari, via Orabona 4, I-70126, Bari, Italy. E-mail: d.cozzoli@ba.ipcf.cnr.it; Fax: +39 080 5442129; Tel: +30 080 5442027*
[b]*CNR-IPCF sez. Bari, c/o Dipartimento di Chimica, Università di Bari, via Orabona 4, I-70126, Bari, Italy. Tel: +39 080 5442027*

Notes and references

1 M. A. El-Sayed, *Acc. Chem. Res.*, 2004, **37**, 326.
2 A. P. Alivisatos, *J. Phys. Chem.*, 1996, **100**, 13226.
3 M. R. Hoffmann, S. T. Martin, W. Choi and D. W. Bahnemann, *Chem. Rev.*, 1995, **95**, 69.
4 B. O'Regan and M. Gratzel, *Nature*, 1991, **353**, 737.
5 (*a*) J. Li, Y. Yamada and Y. Nakato, *Chem. Commun.*, 2001, 2170; (*b*) S. Chen and R. W. Murray, *J. Phys. Chem. B*, 1999, **103**, 9996; (*c*) A. C. Templeton, J. J. Pietron, R. W. Murray and P. Mulvaney, *J. Phys. Chem. B*, 2000, **104**, 564; (*d*) S. D. Jhaveri, D. A. Lowy, A. W. Snow, M. G. Ancona and M. L. Tender, *Chem. Commun.*, 2002, 1544.
6 S. Chen, R. S. Ingram, M. J. Hostetler, J. J. Pietron, R. W. Murray, T. G. Schaaff, J. T. Khoury, M. M. Alvarez and R. L. Whetten, *Science*, 1998, **280**, 2098.
7 T. Ung, D. Dunstan, M. Giersig and P. Mulvaney, *Langmuir*, 1997, **13**, 1773.
8 B. I. Ipe, K. George Thomas, S. Barazzouk, S. Hothandani and P. V. Kamat, *J. Phys. Chem. B.*, 2002, **106**, 18.
9 (*a*) T. Ung, L. M. Liz-Marzan and P. Mulvaney, *J. Phys. Chem. B*, 1999, **103**, 6770; (*b*) N. R. Jana, T. K. Sau and T. Pal, *J. Phys. Chem. B*, 1999, **103**, 115; (*c*) T. K. Sau, A. Pal and T. Pal, *J. Phys. Chem. B*, 2001, **105**, 9266.
10 (*a*) P. V. Kamat, *J. Phys. Chem B*, 2002, **106**, 7729; (*b*) P. V. Kamat, *Pure Appl. Chem.*, 2002, **74**, 1963.
11 A. Wood, M. Giersig and P. Mulvaney, *J. Phys. Chem. B*, 2001, **105**, 8810.
12 V. Subramanian, E. E. Wolf and P. V. Kamat, *J. Phys. Chem. B*, 2003, **107**, 7479.
13 (*a*) M. Jacob, H. Levanon and P. V. Kamat, *Nano Lett.*, 2003, **3**, 353; (*b*) V. Subramanian, E. E. Wolk and P. V. Kamat, *J. Am. Chem. Soc.*, 2004, **126**, 4943.
14 (*a*) T. Hirakawa and P. V. Kamat, *Langmuir*, 2004, **20**, 5645; (*b*) T. Hirakawa and P. V. Kamat, *J. Am. Chem. Soc.*, 2005, **127**, 3928.
15 P. D. Cozzoli, E. Fanizza, R. Comparelli, M. L. Curri, D. Laub and A. Agostiano, *J. Phys. Chem. B*, 2004, **108**, 9623.
16 P. D. Cozzoli, A. Kornowski and H. Weller, *J. Am. Chem. Soc.*, 2003, **125**, 14539.
17 P. D. Cozzoli, R. Comparelli, E. Fanizza, M. L. Curri, A. Agostiano and D. Laub, *J. Am. Chem. Soc.*, 2004, **126**, 3868.
18 P. D. Cozzoli, E. Fanizza, M. L. Curri, D. Laub and A. Agostiano, *Chem. Commun.*, 2005, 942.
19 (*a*) P. V. Kamat, I. Bedja and S. Hotchandani, *J. Phys. Chem.*, 1994, **98**, 9137; (*b*) K. Vinodgopal, I. Bedja, S. Hotchandani and P. V. Kamat, *Langmuir*, 1994, **10**, 1767; (*c*) A. Safrany, R. Gao and J. Rabani, *J. Phys. Chem. B*, 2000, **104**, 5848.
20 (*a*) W. Choi and M. R. Hoffmann, *Environ. Sci. Technol.*, 1997, **31**, 89; (*b*) W. Choi and M. R. Hoffmann, *J. Phys. Chem.*, 1996, **100**, 12161; (*c*) J. Stark and J. Rabani, *J. Phys. Chem. B*, 1999, **103**, 8524.